THE JOURNAL OF BIOLOGICAL CHEMISTRY VOL. 285, NO. 10, pp. 6904–6912, March 5, 2010

The Anti-apoptotic Protein BCL2L1/Bcl-xL Is Neutralized by Pro-apoptotic PMAIP1/Noxa in Neuroblastoma, Thereby Determining Bortezomib Sensitivity Independent of Prosurvival MCL1 Expression*[S]

Received for publication, June 26, 2009, and in revised form, November 27, 2009 Published, JBC Papers in Press, January 5, 2010, DOI 10.1074/jbc.M109.038331

Judith Hagenbuchner[‡§1], Michael J. Ausserlechner[‡¶1], Verena Porto[‡], Reinhard David[‡], Bernhard Meister[¶], Martin Bodner[¶], Andreas Villunger[‖], Kathrin Geiger[‡], and Petra Obexer[‡§2]

From the [‡]Tyrolean Cancer Research Institute, the [§]Department of Pediatrics IV, the [¶]Department of Pediatrics II, and the [‖]Department of Developmental Immunology, Biocenter, Medical University Innsbruck, 6020 Innsbruck, Austria

Neuroblastoma is the most frequent extracranial solid tumor in children. Here, we report that the proteasome inhibitor bortezomib (PS-341, Velcade) activated the pro-apoptotic BH3-only proteins PMAIP1/Noxa and BBC3/Puma and induced accumulation of anti-apoptotic MCL1 as well as repression of anti-apoptotic BCL2L1/Bcl-xL. Retroviral expression of Bcl-xL, but not of MCL1, prevented apoptosis by bortezomib. Gene knockdown of Noxa by shRNA technology significantly reduced apoptosis, whereas Puma knockdown did not affect cell death kinetics. Immunoprecipitation revealed that endogenous Noxa associated with both, Bcl-xL and MCL1, suggesting that in neuronal cells Noxa can neutralize Bcl-xL, explaining the pronounced protective effect of Bcl-xL. Tetracycline-regulated Noxa expression did not trigger cell death *per se* but sensitized to bortezomib treatment in a dose-dependent manner. This implies that the induction of Noxa is necessary but not sufficient for bortezomib-induced apoptosis. We conclude that MCL1 steady-state expression levels do not affect sensitivity to proteasome-inhibitor treatment in neuronal tumor cells, and that both the repression of Bcl-xL and the activation of Noxa are necessary for bortezomib-induced cell death.

Neuroblastoma is a neoplasm that develops from undifferentiated precursors of the sympathetic nervous system and is the most common extracranial solid tumor in childhood. Whereas low stage and local tumors often regress, children older than one year with metastatic, stage IV neuroblastoma face a poor prognosis (1).

The proteasome is a large, multicatalytic enzyme that degrades proteins that are labeled by ubiquitin chains at specific sites. Thereby, the proteasome pathway plays a pivotal role in the regulation of cell cycle and apoptosis. The proteasome inhibitor bortezomib (bort)[3] (PS-341, Velcade), a dipeptidyl-boronic acid is a novel agent that inhibits the proteasome pathway by specifically blocking the chemotryptic enzyme activity of the 20 S complex in the 26 S proteasome (2). Preclinical studies have shown that bortezomib overcomes resistance against standard chemotherapeutic agents and radiation therapy by inducing apoptosis and cell cycle arrest in the G2/M phase. Phase I and II trials on multiple myeloma patients indicate very promising response rates (3) and for relapsed multiple myeloma and mantle cell lymphoma bortezomib has become a standard of care. The toleration with minimal systemic toxicity was also demonstrated for pediatric patients with refractory solid tumors (4).

Programmed cell death can be induced by numerous stimuli such as death ligands, radiation, UV, or growth factor withdrawal, which either activate death receptors on the surface of the cell (extrinsic pathway) or lead to destruction of mitochondria and induction of the intrinsic death pathway (5). Both pathways converge in the activation of effector caspases, which catalyze the final steps of apoptosis. The extrinsic death pathway is initiated by binding of death ligands to surface receptors and subsequent formation of the death-inducing signaling complex (DISC), which consists of receptor molecules, the adaptor FADD and CASP8/caspase-8. Recruitment and autoactivation of caspase-8 lead to the activation of the downstream effector caspases. The intrinsic, mitochondrial pathway is activated either by changes in the balance of BCL2 proteins or by death receptors through cleavage of the pro-apoptotic protein BID. The initiation of the intrinsic pathway results in the release of cytochrome *c* from mitochondria, the assembly of the apoptosome, and subsequent cleavage of effector caspases. The mitochondrial pathway is controlled by members of the BCL2 family, which are divided into three subgroups based on their pro- or anti-apoptotic activities. The multidomain proteins,

* This work was supported by grants from the Kinderkrebshilfe Tirol und Vorarlberg, the Südtiroler Krebshilfe-Vereinigung, the SVP-Frauen-Initiative, the Kinderkrebshilfe Südtirol-Regenbogen, the OeNB Anniversary Fund (Projects 11436 and 12582), and the COMET Center ONCOTYROL. The Tyrolean Cancer Research Institute and this study were supported by the Tiroler Landeskrankenanstalten Ges.m.b.H. (TILAK), the Tyrolean Cancer Society, and by the Dept. of Health-Care, Autonomy of South Tyrol.

[S] The on-line version of this article (available at http://www.jbc.org) contains supplemental Figs. S1–S5.

[1] Both authors contributed equally to this work.

[2] To whom correspondence should be addressed: Pediatric Oncology Research Laboratory, Tyrolean Cancer Research Institute and Dept. of Pediatrics IV, Medical University Innsbruck, Innrain 66, A-6020 Innsbruck, Austria. Tel.: 0043-512-570485-49; Fax: 0043-512-570485-44; E-mail: Petra.Obexer@i-med.ac.at.

[3] The abbreviations used are: bort, bortezomib; doxy, doxycycline; EGCG, *epi*-gallochatechin gallate; CHAPS, 3-[(3-cholamidopropyl)dimethylammonio]-1-propanesulfonic acid; FACS, fluorescent-activated cell sorting; PI, propidium iodide; GAPDH, glyceraldehyde-3-phosphate dehydrogenase.

such as the pro-apoptotic proteins BAX and BAK1/Bak contain three and the anti-apoptotic proteins BCL2, BCL2L1/Bcl-xL, BCL2L2/Bcl-w, BCL2A1/A1, and MCL1 four BCL2 homology (BH) domains (5, 6). The anti-apoptotic activity of BCL2 and its relatives is counteracted by pro-apoptotic BH3-only proteins such as BBC3/Puma, PMAIP1/Noxa,[4] and BCL2L11/Bim, which contain only one BH-domain, *i.e.* the BH3-domain, and serve as triggers for the apoptotic signal. Oligomerization of BAX or Bak in the mitochondrial outer membrane finally causes cytochrome *c* release from mitochondria, which then binds to APAF1 and activates CASP9/caspase-9.

In different cancer cell lines bortezomib treatment was associated with the induction of the BH3-only proteins Noxa, Bim, or BIK (7–9), whereas the expression of pro-survival BCL2 and Bcl-xL was not affected. Although bortezomib inhibits growth of neuroblastoma tumors (10, 11), the underlying molecular mechanisms have not been investigated to date. Because cell death pathways activated by a given substance are often cell type-dependent we investigated the molecular basis of bortezomib-induced apoptosis in neuroblastoma cells.

EXPERIMENTAL PROCEDURES

Cell Lines and Reagents—The neuroblastoma cell lines SH-EP, LAN-1 (kindly provided by Dr. N Gross, Pediatric Oncology Research, Pediatric Department, University Hospital CHUV, Lausanne, Switzerland), SKNSH, SH-SY5Y (purchased from the American Type Culture Collection, ATCC), IMR-32 (purchased from the DSMZ, Braunschweig, Germany) and the neuroblastoma cells STA-NB1, STA-NB3, and STA-NB15 (kindly provided by Dr. P. Ambros, St. Anna Children's Hospital, Vienna,) were cultured in RPMI1640 (PAA, Pasching, Austria) containing 10% fetal calf serum (Invitrogen, Paisley, GB), 100 units/ml penicillin, 100 μg/ml streptomycin, and 2 μM L-glutamine at 5% CO_2 and 37 °C in saturated humidity. All cultures were routinely tested for mycoplasma contamination. The pan-caspase-inhibitor (zVAD.fmk) was purchased from Alexis (San Diego, CA).

Retroviral Expression Constructs—The retroviral vectors pLIB-MCS2-iresPuro, pLIB-dnFADD-iresPuro, pQ-tetH1-SV40Puro, pQ-tetH1-shNoxa-SV40Puro, and pLIB-rtTAM2-iresTRSID-iresPuro have been described before (12, 13). The coding regions of Bcl-xL, CrmA, and MCL1 were amplified from cDNA, inserted into the EcoR1-BamH1 sites of pLIB-MCS2-iresPuro and verified by sequencing. For conditional gene expression, the coding region of Noxa was amplified from human cDNA. The fragment was inserted into the EcoR1-BamH1 sites of the tet-regulated expression vector pQ-tetCMV-SV40-Neo generating the plasmid pQ-tetCMV-Noxa-SV40-Neo.

Retroviral Infection—6×10^5 Phoenix^{TM} packaging cells were transfected with 2 μg of retroviral vector and 1 μg of a plasmid coding for VSV-G protein using Lipofectamine2000 (Invitrogen). After 48 h, the retrovirus-containing supernatants were filtered through 0.2-μm syringe filters (Sartorius, Germany) and incubated with target cells for another 8 h. Cells were infected with pLIB-Bcl-xL-iresPuro (SH-EP-BclxL, NB15-BclxL), pLIB-CrmA-iresPuro (SH-EP-CrmA), pLIB-dnFADD-iresPuro (SH-EP-dnFADD), pLIB-Mcl1-iresPuro (SH-EP-Mcl1, NB15-Mcl1), pQ-tetH1-shNoxa-SV40Puro (SH-EP-shNoxa) pQ-tetH1-SV40Puro (SH-EP-shCtr), and pMSCV-PUMA2-SV40Puro (14) (SH-EP-shPuma). For tetracycline-regulated gene expression, SH-EP cells were infected with pLIB-rtTAM2-iresTRSID-iresPuro (SH-EP-tetCtr (13)). Bulk-selected cells were infected with pQ-tetCMV-Noxa-SV40-Neo (SH-EP-tetNoxa) and selected with neomycin.

Proteasomal Activity—The activity of the proteasome in cell lysates and of cells treated with bortezomib was assessed using a 20 S proteasome assay kit (Cayman Chemicals Company, Ann Arbor, MI) according to the manufacturer's instruction.

Flow Cytometry—Apoptosis was assessed by staining the cells with propidium iodide (PI) as described before (15). Caspase-3 and -9 activation was detected using a caspase-3- or caspase-9 detection kit from Calbiochem (La Jolla, CA), respectively. Bortezomib-treated and untreated SH-EP cells were harvested and incubated for 1 h at 37 °C with FITC-DEVD-FMK dilution according to the manufacturer's protocol. Mitochondrial membrane potential was measured by the fluorescence dye Mitotracker red/CMX-Ros (Invitrogen) according to the manufacturer's instructions. Statistical analysis was performed using GraphPad Prism 4.0 software.

Subcellular Fractionation and Immunoblotting—Cytoplasmic and mitochondrial extracts were prepared using the ApoAlert^{R} Cell Fractionation Kit (BD-Clontech). Cell extracts for immunoblot analysis were prepared and separated by SDS-PAGE as described (16). The membranes were incubated with primary antibodies specific for BCL2, Bim, caspase-8, CrmA, MCL1 (BD-Pharmingen, Germany), Bcl-xL, caspase-9, A1 (Cell Signaling Technology), FADD, Noxa (Alexis Biochemicals, Switzerland), Puma (Sigma-Aldrich), cytochrome *c* (BD-Clontech), GAPDH (Novus Biologicals), and α-tubulin (Oncogene Research Products), washed, and incubated with anti-mouse or anti-rabbit horseradish peroxidase-conjugated secondary antibodies. The blots were developed using ECL (GE-Healthcare) and analyzed in an AutoChemi system (UVP, GB).

Co-immunoprecipitation Analyses—For immunoprecipitation, 2 μg of rabbit anti-Bcl-xL (Cell Signaling, UK), 2 μg of rabbit anti-MCL1 (BD-Pharmingen, Germany) or rabbit immunoglobulin as negative control were covalently coupled to Tachisorb^{TM}-immunoadsorbent (Calbiochem). For coupling, beads were washed twice with phosphate-buffered saline and were then incubated with antibodies for 1 h at room temperature. After centrifugation, beads were washed twice with coupling buffer (0.1 M borax/boric acid, pH 9.0) and with dimpim buffer (0.05 g of dimethylpimelidate dihydrochloride (Sigma) dissolved in 0.1 M borax pH 9) and incubated overnight at 4 °C in dimpim buffer. For precipitation, beads were equilibrated in lysis buffer. 5×10^7 cells were either resuspended in MSH buffer (210 mM mannitol, 70 mM sucrose, 20 mM HEPES, 1 mM EDTA, pH 7.4) with 1% CHAPS (for Bcl-xL) or in 1% Nonidet P-40-buffer (for MCL1) with protease and phosphate inhibitors and left on ice for 1 h. Nuclei and non-lysed cells were removed by centrifugation at 14,000 $\times$ *g* for 15 min. The protein concentration was measured using Bradford Reagent. For pull-down,

[4] Following a recommendation by the HUGO Gene Nomenclature Committee all official human gene symbols are put in uppercase letters to distinguish them from their often more widely used aliases, e.g. *PMAIP1* is *Noxa*.

coupled antibodies were added for 6 h and rotated at 4 °C. Tachisorb™ immunocomplexes were washed four times in Nonidet P-40 or MSH buffer before being resuspended in SDS sample buffer and subjected to SDS-PAGE. For immunoblot detection, the membranes were incubated with primary antibodies specific for Bcl-xL (Cell Signaling Technology), or MCL1 (BD-Pharmingen).

Quantitative RT-PCR—Total RNA was prepared from 5×10^6 SH-EP and STA-NB15 cells using TRIzol™ reagent (Invitrogen) according to the manufacturer's instructions. cDNA synthesis was performed using the RevertAid™ First Strand cDNA Synthesis kit (MBI Fermentas, Germany). RT-PCR was performed on the iCycler instrument (Bio-Rad) using Noxa (forward AGCAGAGCTGGAAGTCGAGTGTG and reverse TGATGCAGTCAGGTTCCTGAGC), Puma (forward ACGACCTCAACGCACAGTACGAG and reverse TAATTGGGCTCCATCTCGGG), and GAPDH (forward TGTTCGTCATGGGTGTGAACC and reverse GCAGTGATGGCATGGACTGTG) primers. After normalization on GAPDH expression, regulation was calculated between treated and untreated cells.

RESULTS

The Proteasome Inhibitor Bortezomib Induces Apoptotic Cell Death in Human Neuroblastoma Cells—As the plasma concentration of patients treated with 1.3 mg of bortezomib per m^2 body surface reaches about 300 nM, we chose doses between 12 and 100 nM to assess neuroblastoma sensitivity *in vitro* and exposed a set of different neuroblastoma cell lines to bortezomib for 24 and 48 h. SH-EP, Lan-1, SKNSH, SH-SY5Y, IMR-32, STA-NB1, STA-NB3, and STA-NB15 cells showed a time- and dose-dependent susceptibility to the proteasome inhibitor (Fig. 1, *A* and *B*). Cell lines varied in their sensitivity to these concentrations of the proteasome inhibitor: Whereas 85% of SH-EP cells became apoptotic after 48 h of treatment with 100 nM bortezomib, in other cell lines such as STA-NB1 only about 35% of cells exposed to as much as 100 nM bortezomib underwent programmed cell death. For further detailed analysis of the involved apoptosis signaling pathways we therefore chose caspase-8-expressing SH-EP and caspase-8-negative STA-NB15 cells. To test whether these relatively low concentrations of bortezomib exert an inhibitory effect on protein degradation via the proteasome pathway the proteasomal activity was measured *in vitro* using a fluorescence-based proteasome activity assay. Bortezomib (50 nM) was either used to treat SH-EP cells for 8 h (bort*) or directly added to SH-EP cell lysates (bort). In both cases 50 nM bortezomb significantly ($p < 0.0001$) reduced proteasome activity to less than 35% of controls. The inhibitor EGCG was provided by the manufacturer and used as a positive control (Fig. 1*C*).

Bortezomib-induced Apoptosis Critically Involves Caspases and the Mitochondrial Death Pathway—We next determined mitochondrial activity by Mitotracker red/CMX-Ros staining and the presence of cytochrome *c* in the cytoplasmic fraction by subcellular fractionation assays. Bortezomib decreased mitochondrial activity (Fig. 2*A*), and the amount of CMX-Ros-negative cells was increased by bortezomib from 6.7 to 88% within 48 h. Furthermore cytoplasmic cytochrome *c* was induced by

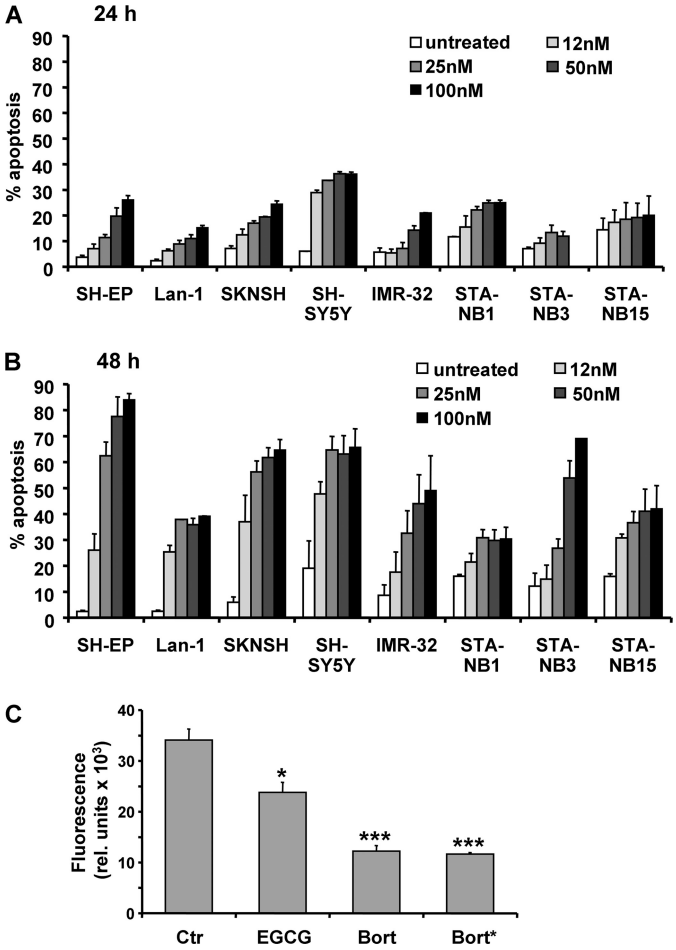

FIGURE 1. **The proteasome inhibitor bortezomib induces apoptosis in various neuroblastoma cell lines.** The neuroblastoma cell lines SH-EP, Lan-1, SKNSH, SH-SY5Y, IMR-32, STA-NB1, STA-NB3, and STA-NB15 were treated with increasing doses of bortezomib (12, 25, 50, 100 nM) for 24 (*A*) and 48 h (*B*) and analyzed by PI-FACS analyses. *C*, proteasomal activity was analyzed using a fluorescence-based proteasome activity assay. SH-EP cells were either treated with 50 nM bortezomib for 8 h and then subjected to proteasome preparation (bort*) or lysates of untreated SH-EP cells were directly incubated with 50 nM bortezomib (bort) or the proteasome inhibitor EGCG. Statistical significance between control and treated samples was assessed by the unpaired Student's *t* test (*, $p < 0.05$; ***, $p < 0.0001$).

1.6-fold during 24 h in the presence of bortezomib (Fig. 2*B*). Because caspase-8 and caspase-9 are initiator caspases of the extrinsic and intrinsic pathway, respectively, we examined the presence of characteristic cleavage products in bortezomib-treated cells by immunoblot analysis (Fig. 2*C*). Caspase-9 cleavage was detected in SH-EP cells after 16 h and in STA-NB15 cells after 24 h, suggesting early activation of the mitochondrial death pathway. Because STA-NB15 cells lack caspase-8 (12) only SH-EP cells were analyzed for caspase-8-cleavage. Caspase-8 processing was delayed, and cleavage fragments were first detected after 24 h of bortezomib treatment, indicating that caspase-8 cleavage was a secondary consequence of activation of the caspase-9/caspase-3 axis. To assess the kinetics of caspase-3 activation, SH-EP and STA-NB15 cells were treated for 24 and 48 h with 50 nM bortezomib and active caspase-3 was quantified by a fluorometric caspase-3 cleavage assay and flow cytometry (Fig. 2*D*). A strong increase of fluorescence intensity was detected between 24 and 48 h of bort-

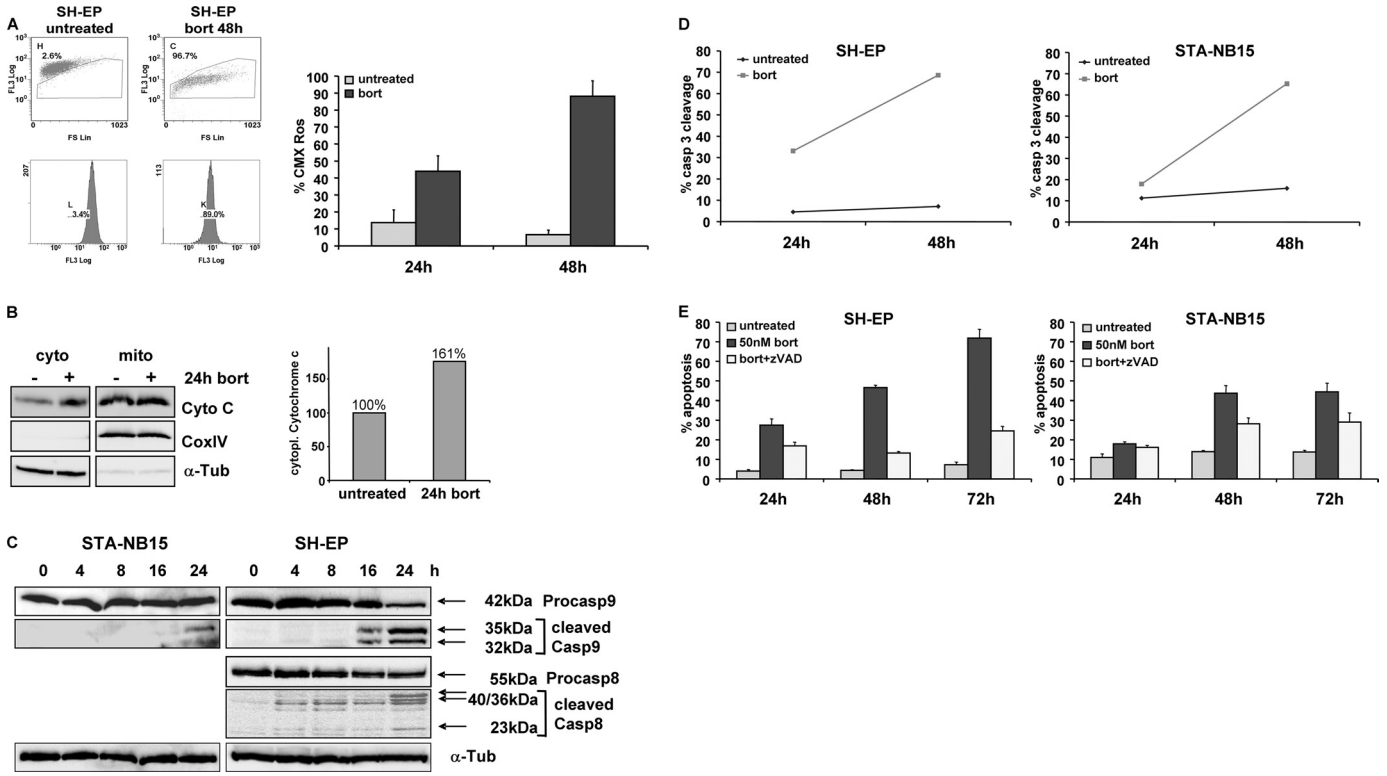

FIGURE 2. **Bortezomib-induced apoptosis requires caspase activation and involves mitochondria.** *A*, mitochondrial activity was measured by CMX-Ros staining of SH-EP cells in the presence or absence of 50 nM bortezomib for 48 h. *B*, cytoplasmic cytochrome *c* of untreated and 24 h bortezomib-treated SH-EP cells was detected by immunoblot, and the amount of cytoplasmic cytochrome *c* was measured by densitometry of 16-bit images using LabWorks software. *C*, STA-NB15 and SH-EP cells were treated with 50 nM bortezomib for 0, 4, 8, 16, and 24 h. Cell lysates were subjected to immunoblot analyses using specific antibodies against caspase-9 (with cleavage products of 35 and 32 kDa) and caspase-8 (cleavage products of 40, 36, and 23 kDa). α-Tubulin was used as loading control. *D*, active caspase-3 was detected by the fluorogenic FITC-DEVD.fmk substrate of the caspase-3 cleavage assay in the cells SH-EP and STA-NB15 after treatment with 50 nM bortezomib (bort) for 24 and 48 h. *E*, SH-EP and STA-NB15 cells were maintained for 24, 48, and 72 h in the presence of 50 nM bortezomib alone or in combination with z-VAD, a pan-caspase-inhibitor (20 nM), and subjected to PI-FACS analyses. Diagrams represent mean values of three independent experiments.

ezomib treatment. Co-treatment with the pan-caspase-inhibitor zVAD.fmk (20 nM) reduced the level of bortezomib-induced apoptosis from 47 to 13% after 48 h and from 72 to 24% after 72 h in SH-EP cells. The same inhibitory effect of zVAD.fmk, although less pronounced, was observed in STA-NB15 cells (Fig. 2*E*). This suggests that the activation of caspases is critical for the execution of bortezomib-induced apoptosis but that other death pathways can be activated when apoptosis is blocked (17). The combined data suggest that bortezomib induces apoptotic cell death via mitochondria and caspase activation in neuroblastoma cells. Because caspase-8 cleavage was also observed in SH-EP cells, and immunoblot analyses cannot be used to define unambiguously the activation sequence of caspases, we investigated whether activation of death receptors and/or amplification via caspase-8 might contribute to bortezomib-induced apoptosis execution in neuroblastoma cells.

Death Receptors Are Not Essential for Bortezomib-induced Apoptosis—To support or exclude the hypothesis that death receptors act as initial triggers in bortezomib-induced apoptosis, SH-EP neuroblastoma cells were infected with a retrovirus coding for dominant negative FADD (dnFADD) (12) or the viral caspase-8 inhibitor CrmA (Fig. 3*A*). Both, transgenic expression of dnFADD and CrmA efficiently prevented death receptor-induced apoptosis as triggered by the anti-Fas antibody CH11 (supplemental Fig. S1). However, neither dnFADD nor CrmA significantly altered apoptosis induced by 50 nM bortezomib (Fig. 3*B*). Therefore, although activation of caspase-8 was detectable 24 h after bortezomib treatment (Fig. 2*C*), death receptor signaling is not critical for apoptosis.

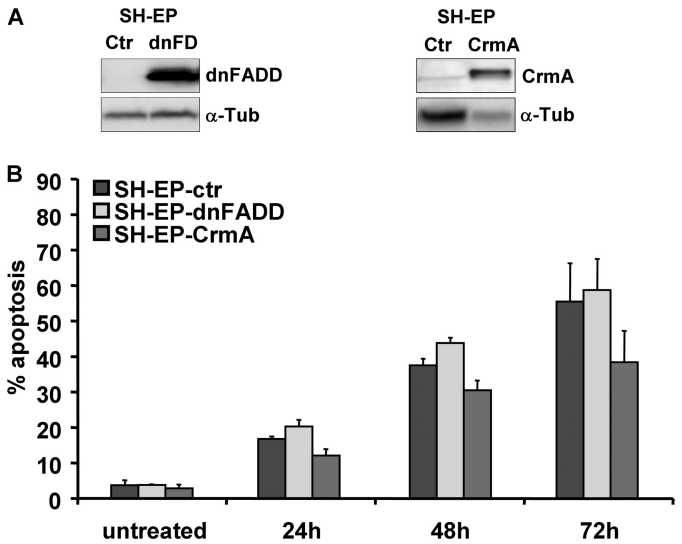

FIGURE 3. **Death receptors are not essential for bortezomib-induced cell death.** *A*, SH-EP cells were infected with retroviral vectors coding for dnFADD and CrmA. The transgenic expression was confirmed by immunoblot. *B*, SH-EP-ctr, SH-EP-dnFADD, and SH-EP-CrmA cells were subjected to PI-FACS analyses after treatment with 50 nM bortezomib for 24, 48, and 72 h. *Bars* represent the mean of three independent experiments.

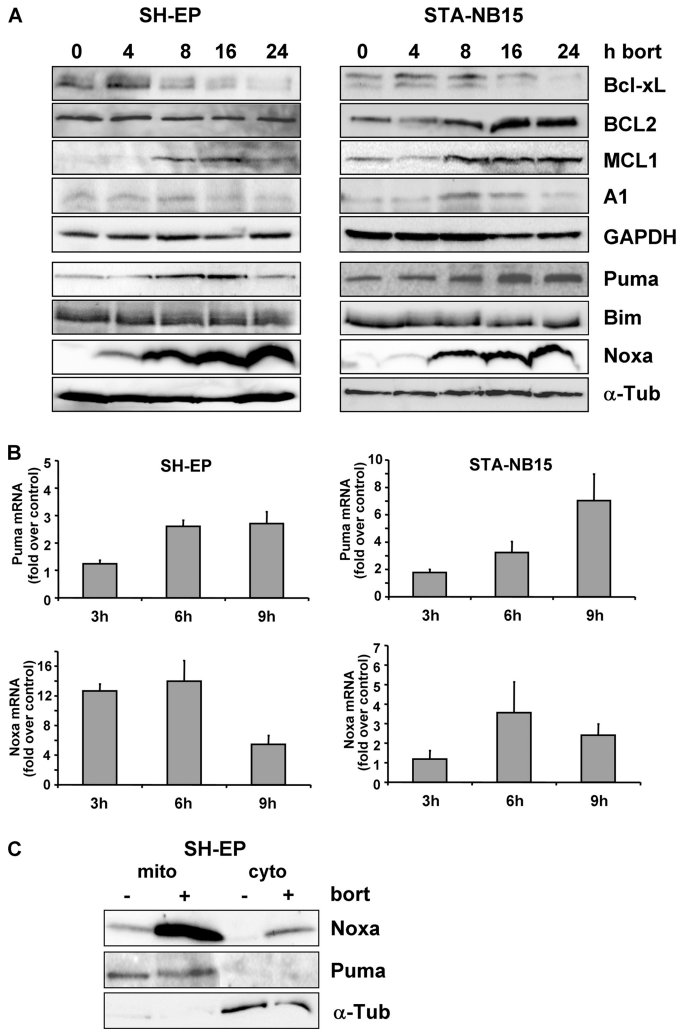

FIGURE 4. **Bortezomib causes up-regulation of Noxa, Puma, and MCL1 and repression of Bcl-xL.** *A*, SH-EP and STA-NB15 cells were subjected to immunoblot analyses using antibodies against BCL2, Bcl-xL, A1, MCL1, Puma, Bim, and Noxa after treatment with 50 nM bortezomib for 0, 4, 8, 16, and 24 h. α-Tubulin and GAPDH were used as loading controls. *B*, total RNA was prepared from SH-EP and STA-NB15 cells after treatment with 50 nM bortezomib for 0, 3, 6, and 9 h and the level of Puma and Noxa mRNA was assessed by quantitative RT-PCR (mean values of three independent experiments, each performed in triplicate). *C*, subcellular fractionation of untreated and 50 nM bortezomib-treated (24 h) SH-EP cells. Mitochondrial (*mito*) and cytoplasmic (*cyto*) fractions were subjected to immunoblot analyses of Noxa, Puma, and α-tubulin.

This suggests that caspase-8 may contribute to cell death execution, but is activated downstream of mitochondrial cytochrome *c* release and independent of death receptors (18, 19). We therefore next assessed the mRNA and protein expression of pro- and anti-apoptotic BCL2 proteins.

Differential Regulation of BCL2 Family Members in Bortezomib-treated Neuroblastoma—SH-EP and STA-NB15 cells were treated for 0, 4, 8, 16, and 24 h with 50 nM bortezomib and then subjected to immunoblot analyses. Bortezomib therapy repressed Bcl-xL and induced accumulation of MCL1 in both cell lines and expression of BCL2 and A1 only in STA-NB15 cells (Fig. 4*A*). MCL1 is degraded via the proteasome and stabilized in response to bortezomib treatment (20). The repression of Bcl-xL by bortezomib in neuroblastoma occurred both on mRNA (supplemental Fig. S2) and protein steady-state level and was not shown before. The pro-survival activity of BCL2, Bcl-xL, A1, and MCL1 is counteracted by pro-apoptotic BH3-only proteins, such as Bim, Puma, and Noxa. Bim steady-state protein expression was unaffected, whereas Noxa and to a lesser extent also Puma protein levels increased in response to bortezomib in both neuroblastoma cell lines (Fig. 4*A*). Puma was induced 3-fold after 6 h in SH-EP cells as measured by quantitative RT-PCR. In STA-NB15 cells Puma mRNA was 3-fold induced after 6 h and 7-fold elevated after 9 h of bortezomib treatment. Similar to protein level, bortezomib also strongly induced Noxa mRNA: Noxa was 12- and 14-fold induced after 3 and 6 h, respectively, whereas at 9 h post-addition of bortezomib Noxa-mRNA levels decreased in SH-EP cells (Fig. 4*B*). The same phenomenon of transient induction was also observed in STA-NB15 cells. This mRNA steady-state regulation was in contrast to the continuous increase of Noxa protein up to 24 h. It suggests that both, transcriptional and post-translational effects of bortezomib contribute to the marked elevation of cellular Noxa expression as shown in Fig. 4*A*. To determine the subcellular localization of Noxa and Puma in untreated or bortezomib-treated SH-EP cells we performed subcellular fractionation assays and found that Noxa, like Puma, predominantly co-purified with the membrane fraction (Fig. 4*C*). A small amount of Noxa was also found in the cytoplasmic fraction of bortezomib-treated cells, suggesting that the increase of Noxa even might exhaust the binding capacity of mitochondrial Noxa binding partners.

Bcl-xL Protects against Apoptosis by Bortezomib—To functionally assess whether the above observed changes in pro-survival and pro-apoptotic BCL2 proteins are relevant for apoptosis decision we generated a set of constitutive cell lines that overexpress distinct BCL2 family members. Retroviral vectors coding for Bcl-xL, MCL1, and BCL2 (supplemental Fig. S3) were infected into SH-EP and STA-NB15 cells (Fig. 5*A*). Mock-infected cell lines were used as controls. Bcl-xL and to a lesser extent also BCL2 exerted a significant protective effect to death by proteasome inhibition. In STA-NB15 cells transgenic Bcl-xL even completely prevented bortezomib-induced apoptosis. This suggests that down-regulation or functional inactivation of Bcl-xL is essential for the onset of apoptosis by bortezomib. Surprisingly, retroviral overexpression of MCL1 did not markedly affect bortezomib-induced apoptosis up to 72 h in SH-EP-Mcl1 and NB15-Mcl1 cells as shown in Fig. 5*A* (*lower panels*). In contrast, transgenic MCL1 significantly reduced Fas-, TRAIL-, and doxorubicin-induced cell death in SH-EP cells (supplemental Fig. S4). This suggests that either the induction of Noxa cannot be effectively antagonized by MCL1 levels present in the cell or that Noxa may neutralize other pro-survival members of the BCL2 family in addition to MCL1. To study whether the protective effect of Bcl-xL may be ascribed to sequestration by Noxa, we precipitated MCL1 and Bcl-xL from bortezomib-treated or untreated NB15-BclxL cells, because these cells are fully protected against apoptosis and loss of Bcl-xL is prevented by transgenic expression. As shown in Fig. 5*B*, Noxa co-purified with both, MCL1 and Bcl-xL, although the latter was unexpected due to its reported low affinity for Noxa (21). Transgenic Bcl-xL slightly accumulated during bortezomib treatment con-

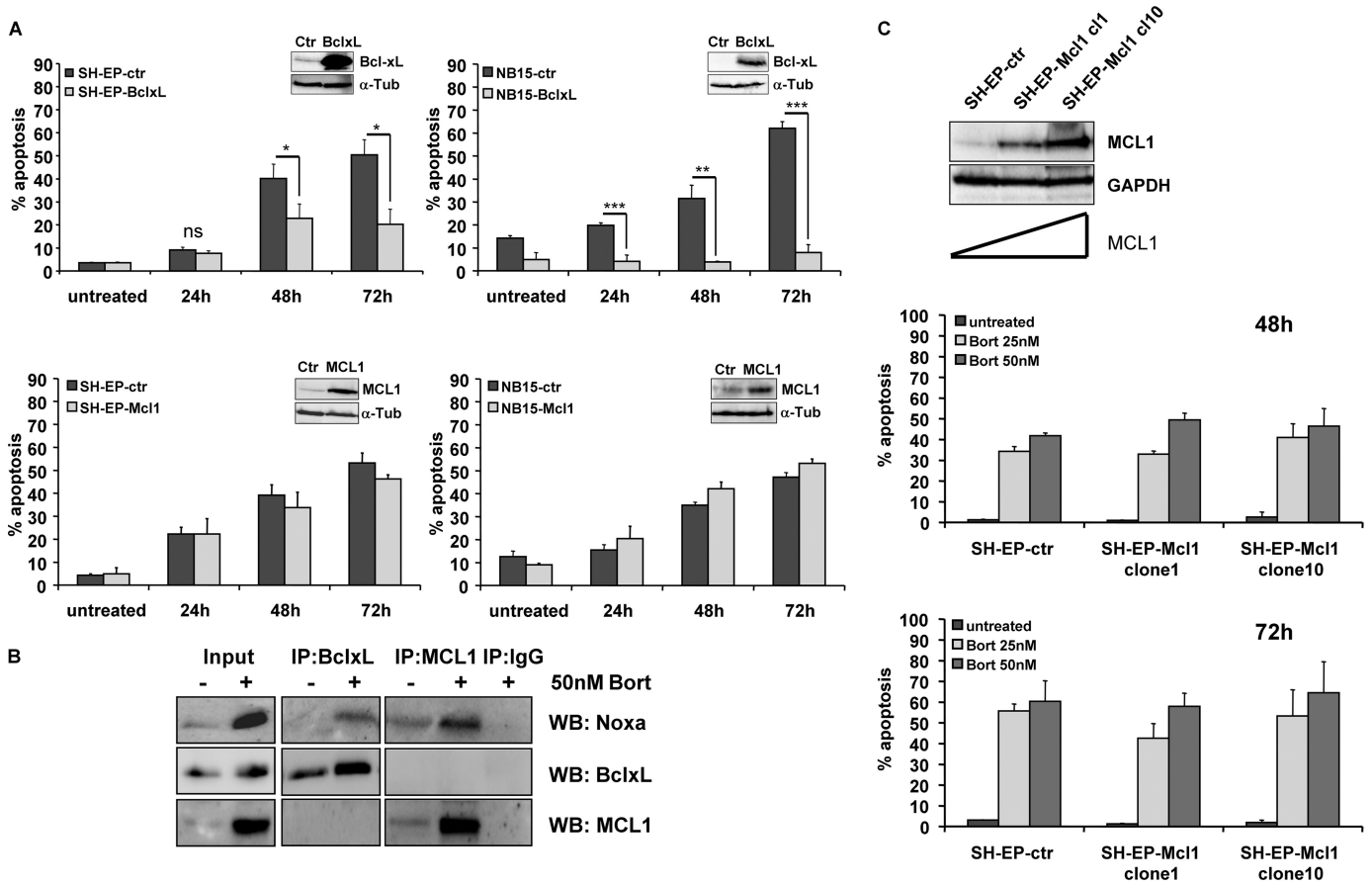

FIGURE 5. **Transgenic Bcl-xL is neutralized by Noxa and inhibits bortezomib-induced apoptosis, whereas MCL1 has no impact on death sensitivity.** *A*, SH-EP and STA-NB15 cells were retrovirally infected with vectors coding for Bcl-xL and MCL1. The ectopic expression was verified by immunoblot analysis. Cells were treated with 50 nM bortezomib for the times indicated and subjected to PI-FACS analyses. Statistical significance between mock-infected controls and Bcl-xL transgenic cells was assessed by the unpaired Student's *t* test (*, $p < 0.05$; ***, $p < 0.001$). *B*, NB15-BclxL cells were treated for 18 h with 50 nM bortezomib, lysed, and subjected to co-immunopurification using rabbit anti-MCL1 and rabbit anti-Bcl-xL as precipitating antibodies, rabbit IgG was used as negative control. Immunoprecipitates were analyzed for presence of Noxa, Bcl-xL, and MCL1 by immunoblot. *C*, single cell clones were isolated by limiting dilution from SH-EP-Mcl1 cells. MCL1 expression in mock-infected SH-EP-ctr, SH-EP-Mcl1 clone1, and clone10 cells was determined by immunoblot analysis. SH-EP-ctr, SH-EP-Mcl1 clone1, and clone10 cells were treated with 25 and 50 nM bortezomib and subjected to PI-FACS analysis for 48 and 72 h.

sistent with efficient inhibition of proteasomal activity shown in Fig. 1*C*. To investigate whether the lack of protection by transgenic MCL1 from bortezomib-induced apoptosis in bulk cultures was due to insufficient levels of MCL1, we studied drug-induced cell death in individual clones expressing low, intermediate or high levels of MCL1. As shown in Fig. 5*C*, varying MCL1 steady-state expression did not alter responsiveness to bortezomib in SH-EP cells. This suggests that MCL1 levels do not critically affect bortezomib sensitivity in neuronal cells but that the gradual decline of Bcl-xL is required for cell death to occur.

Noxa but Not Puma Is Rate Limiting for Bortezomib-induced Apoptosis in Neuroblastoma Cells—To directly assess whether Noxa or Puma are critical for cell death by proteasome inhibition, we stably knocked down Noxa and Puma by shRNA technology using retroviral vectors for the expression of Noxa- (12) or Puma-specific shRNA (14, 22). Individual clones were analyzed by immunoblot for Noxa or Puma expression, respectively (Fig. 6*A*), and the number of apoptotic cells was quantified by flow cytometry (Fig. 6*B*). The knockdown of Noxa resulted in a significant reduction of basal Noxa protein levels compared with mock-infected cells and decreased apoptosis after 24 h of bortezomib treatment from 41 to 12% ($p = 0.0002$) and 7% ($p < 0.0001$), respectively. In contrast, knockdown of endogenous Puma did not affect bortezomib-induced cell death at all (Fig. 6*B*, *right panel*). To study whether the knockdown of Noxa hampers cell death activation at the level of mitochondria, we assessed cleavage of caspase-9 by a fluorometric caspase-9 cleavage assay (Fig. 6*C*). Whereas about 50% of SH-EP-shCtr cells became positive for active caspase-9 after 24 h in the presence of 50 nM bortezomib, Noxa knockdown significantly reduced this percentage to less than 20% ($p = 0.005$, Fig. 6*C*). These results indicate that Noxa is rate limiting for bortezomib-induced apoptosis, whereas Puma does not affect cell death by proteasome inhibition in human neuroblastoma cells.

Noxa Expression Levels Determine Sensitivity to Bortezomib-induced Apoptosis—To assess whether Noxa steady state levels determine death sensitivity to bortezomib, we used a recently developed tetracycline-regulated, retroviral expression system (13) for conditional expression of Noxa in bulk-selected SH-EP cells. Doxycycline (doxy)-induced expression of Noxa was verified by immunoblotting and cell death was assessed by FACS analysis of PI-stained nuclei (Fig. 6*D*). Consistent with the observation that Noxa is a weak death agonist (23, 24) even

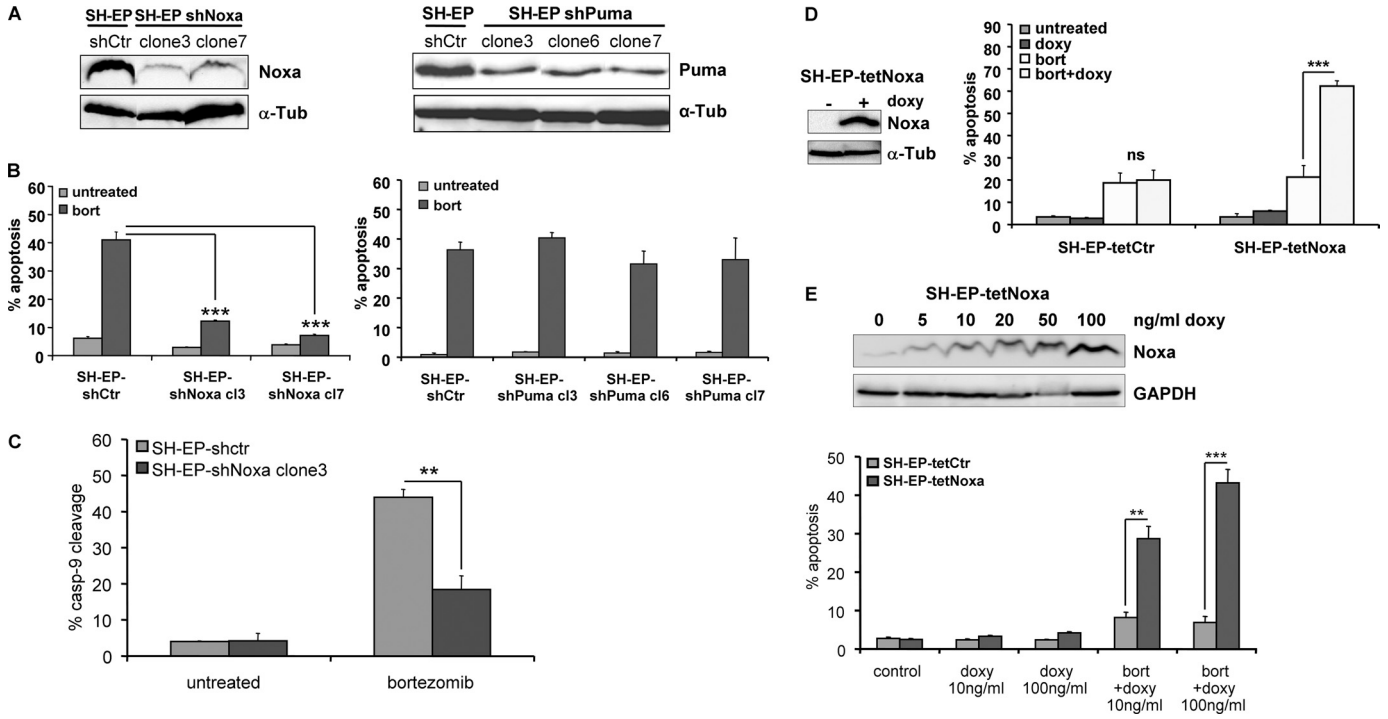

FIGURE 6. **Noxa is rate limiting for bortezomib-induced apoptosis.** *A*, SH-EP cells were infected with retroviruses expressing shRNA specific for Noxa or Puma. Individual clones were isolated from bulk-selected SH-EP-shNoxa and SH-EP-shPuma cells and steady-state expression level of endogenous Noxa (*left panel*) or Puma (*right panel*) was verified by immunoblot analysis. *B*, cell lines SH-EP-shCtr and SH-EP-shNoxa clone 3 and clone 7 as well as SH-EP shPuma clone 3, clone 6, and clone 7 were treated with 50 nM bortezomib for 24 h and subjected to PI-FACS analyses. *C*, SH-EP-shctr and SH-EP-shNoxa clone 3 cells were treated with 50 nM bortezomib for 24 h. Caspase-9 cleavage was determined using a fluorometric caspase activity assay and flow cytometry. Shown is the mean of three independent experiments. Statistics were calculated with GraphPad Prism software using the unpaired Student's *t* test (**, $p = 0.005$; ***, $p < 0.001$). *D*, SH-EP cells designed to express Noxa in a tetracycline-dependent manner were treated with 250 ng/ml doxy for 24 h. Transgene expression was verified by immunoblot analysis. SH-EP-tetCtr, and SH-EP-tetNoxa cells were treated with 250 ng/ml doxy, with 25 nM bortezomib or a combination of both for 24 h and were then subjected to PI-FACS analyses. Shown is the mean of three independent experiments. *E*, to assess a possible dosage-dependent effect of Noxa SH-EP-tetNoxa, cells were treated with 5, 10, 20, 50, and 100 ng/ml doxy and then subjected to immunoblot analysis for Noxa and GAPDH (loading control) expression. SH-EP-tetCtr and SH-EP-tetNoxa cells were treated with 12.5 nM bortezomib in the presence or absence of 10 or 100 ng/ml doxy for 24 h and then subjected to PI-FACS analyses (*bars* represent the mean of three independent experiments). Statistical significance was assessed by the unpaired Student's *t* test (**, $p < 0.01$; ***, $p < 0.001$).

strong expression of Noxa (Fig. 6*D*) did not cause spontaneous cell death after doxy treatment. However, in combination with transgenic Noxa, bortezomib-induced apoptosis increased from 20 to 60% after 24 h ($p = 0.0009$). The utilized tetracycline-regulated expression system allows tightly controlled transgene expression to study gene dosage effects (13) as demonstrated by immunoblot in Fig. 6*E*. PI-FACS analyses of SH-EP-tetCtr and SH-EP-tetNoxa cells treated with low (10 ng/ml) and high (100 ng/ml) concentrations of doxy revealed that bortezomib-induced apoptosis correlated with the cellular amount of Noxa.

DISCUSSION

In this report we analyzed the molecular basis of bortezomib-induced apoptosis in neuroblastoma cells and identified Noxa and Bcl-xL as bortezomib-engaged BCL2 family members that are critical for apoptosis initiation. Bortezomib is clinically used for the treatment of multiple myeloma and mantle cell lymphoma (25) and was also shown to activate cell death in neuroblastoma (10). Because all tested neuroblastoma cell lines were bortezomib-sensitive (Fig. 1), we chose the caspase-8-positive cell line SH-EP and the caspase-8-negative cell line STA-NB15 for further detailed characterization of the molecular death pathway.

Proteasome inhibitors were reported to up-regulate surface death receptors and their ligands (26) implicating them as triggers of cell death. However, retroviral expression of neither dnFADD nor CrmA could block apoptosis suggesting that membrane death receptors are not essential for bortezomib-induced cell death (Fig. 3*B*). Because cleavage products of caspase-8 were detectable after 24 h of bortezomib treatment (Fig. 2*C*), it might participate as an amplifier of cell death execution and contribute to increased bortezomib susceptibility of SH-EP cells compared with caspase-8-negative IMR-32, STA-NB1, STA-NB3, and STA-NB15 cells (Fig. 1, *A* and *B*).

A marked increase of CMX-Ros-negative cells, the release of cytochrome *c* into the cytoplasm and the cleavage of caspase-9 point toward mitochondria as integrators of apoptosis signals during proteasome-inhibition. This is consistent with reports on several other tumor cell types, where activation of the mitochondrial death pathway by bortezomib was described (27). As shown in Fig. 4*A*, in both cell lines anti-apoptotic Bcl-xL decreased whereas MCL1 accumulated. BCL2 and A1 remained unaffected in SH-EP cells but appeared to accumulate in STA-NB15 cells. In parallel, the pro-apoptotic BH3-only proteins Noxa and to a lesser extent Puma were induced on the mRNA and protein level, whereas Bim

levels remained unaffected (Fig. 4, *A* and *B*). Because the transcription factor p53 can be activated in response to proteasome inhibition (28, 29), we also analyzed whether the induction of the p53 target genes Noxa and Puma can be ascribed to p53 activation. In SH-EP cells, p53 was strongly induced by bortezomib and also its target Bax showed transitory elevation whereas in STA-NB15 cells p53 was already detectable in untreated cells and only slightly accumulated upon bortezomib treatment, indicating mutation of this tumor suppressor (supplemental Fig. S5). Nevertheless, in both cell lines Noxa and Puma mRNA expression was induced suggesting that the induction of these pro-apoptotic genes is largely independent of p53 in neuroblastoma cells.

Bcl-xL interacts with all pro-apoptotic members of the BCL2 family and is a direct target of NFκB in neuronal cells (30). Proteasome inhibition stabilizes the NFκB-inhibitor IκB (31), which abrogates NFκB transcriptional activity and might repress the NFκB-target Bcl-xL also in neuronal cells. The loss of Bcl-xL during bortezomib treatment lowers the ability of a cell to cope with high levels of BH3-only death inducers. Importantly, Noxa co-purified with both, MCL1 and Bcl-xL (Fig. 5*B*). Noxa was originally described as a Bcl-xL interaction partner (32) and might thereby at least in part neutralize the pro-survival function of Bcl-xL. Although the affinity between Noxa and Bcl-xL was reported to be lower than *e.g.* between Bim or Puma and Bcl-xL (21) we observed their co-precipitation in bortezomib-treated neuronal cells. The repression of Bcl-xL and its increased sequestration by Noxa might therefore tilt the balance of pro- and anti-apoptotic BCL2 proteins toward death decision. The pronounced effect of transgenic Bcl-xL on apoptosis sensitivity of neuronal cells is also consistent with the phenotype of Bcl-xL knock-out mice that die *in utero* as a consequence of massive neuronal and hematopoietic death (33). The important finding that Noxa and Bcl-xL interact with each other might provide an explanation how Bcl-xL is antagonized in neuronal cells.

High levels of Bcl-xL protect tumor cells against chemotherapy-induced apoptosis (34), and the repression of Bcl-xL by bortezomib might therefore sensitize neuroblastoma cells to chemotherapy, suggesting that in addition to inducing death by its own bortezomib might serve as a chemosensitizing drug. In contrast to Bcl-xL, the pro-survival protein MCL1 accumulated during proteasome inhibition (Fig. 4*A*), and because it is a preferential pro-survival binding partner of Noxa (35), we expected that its elevation counteracts the apoptosis-sensitizing effect of Noxa and slows down bortezomib-induced apoptosis. Surprisingly, transgenic MCL1 neither in bulk-selected cells nor in individual clones with high or intermediate MCL1 expression protected against bortezomib-induced apoptosis although this has been reported for other cancer types (20, 36) and transgenic MCL1 markedly reduced sensitivity to other forms of cell death (supplemental Fig. S4). Therefore, in contrast to Bcl-xL, MCL1 steady-state levels do not affect bortezomib-induced apoptosis in neuroblastoma. This observation in fact might have therapeutic implications for neuroblastoma therapy, because the concordant accumulation of MCL1 during proteasome inhibition is thought to compensate the pro-apoptotic effect of Noxa.

Mitochondrial cell death has mainly been ascribed to the activation of BH3-only proteins, such as Bim, Puma, and Noxa (9, 36). To directly assess the relevance of Noxa and Puma we stably knocked down these proteins by shRNA technology. Although endogenous Puma was markedly reduced in Puma-shRNA-expressing cells (Fig. 6*A*), this did not affect cell death by bortezomib (Fig. 6*B*). This suggests that the Puma accumulation we observed during proteasome inhibition-induced cell death is not critical for apoptosis induction. In contrast, Noxa gene knockdown significantly reduced bortezomib-induced cell death (Fig. 6, *B* and *C*) and conditional Noxa expression sensitized to bortezomib-induced apoptosis in a dose-dependent manner (Fig. 6, *D* and *E*). Gomez-Bougie *et al.* (36) reported that Noxa is essential for bortezomib-induced cell death in multiple myeloma. Our results provide evidence that bortezomib induces apoptosis in neuronal cells by changing the balance of the pro-survival and pro-apoptotic BCL2 proteins Bcl-xL and Noxa. Noxa acts as an apoptosis sensitizer that does not induce death *per se* but its up-regulation and binding to Bcl-xL in concert with gradual loss of Bcl-xL is essential for bortezomib-induced apoptosis irrespective of MCL1 expression levels. Because MCL1 accumulation is an unwanted and compensatory side effect of proteasome inhibitor therapy in other tumor types, this is an important finding of therapeutic value. Thereby, bortezomib might be a promising agent for neuroblastoma treatment, because it induces apoptosis independent of caspase-8/MCL1 status and represses Bcl-xL, which sensitizes neuroblastoma cells for the therapy with chemotherapeutic drugs.

Acknowledgments—We thank Dr. N. Gross and P. Ambros for neuroblastoma cell lines and C. Kitzbichler and M. Wille for excellent technical assistance.

REFERENCES

1. Park, J. R., Eggert, A., and Caron, H. (2008) *Pediatr. Clin. North Am.* **55,** 97–120
2. Adams, J. (2002) *Breast Dis.* **15,** 61–70
3. Jagannath, S., Barlogie, B., Berenson, J., Siegel, D., Irwin, D., Richardson, P. G., Niesvizky, R., Alexanian, R., Limentani, S. A., Alsina, M., Adams, J., Kauffman, M., Esseltine, D. L., Schenkein, D. P., and Anderson, K. C. (2004) *Br. J. Haematol.* **127,** 165–172
4. Blaney, S. M., Bernstein, M., Neville, K., Ginsberg, J., Kitchen, B., Horton, T., Berg, S. L., Krailo, M., and Adamson, P. C. (2004) *J. Clin. Oncol.* **22,** 4804–4809
5. Strasser, A. (2005) *Nat. Rev. Immunol.* **5,** 189–200
6. Chipuk, J. E., and Green, D. R. (2008) *Trends Cell Biol.* **18,** 157–164
7. Pérez-Galán, P., Roué, G., Villamor, N., Montserrat, E., Campo, E., and Colomer, D. (2006) *Blood* **107,** 257–264
8. Zhu, H., Zhang, L., Dong, F., Guo, W., Wu, S., Teraishi, F., Davis, J. J., Chiao, P. J., and Fang, B. (2005) *Oncogene* **24,** 4993–4999
9. Nikrad, M., Johnson, T., Puthalalath, H., Coultas, L., Adams, J., and Kraft, A. S. (2005) *Mol. Cancer Ther.* **4,** 443–449
10. Brignole, C., Marimpietri, D., Pastorino, F., Nico, B., Di Paolo, D., Cioni, M., Piccardi, F., Cilli, M., Pezzolo, A., Corrias, M. V., Pistoia, V., Ribatti, D., Pagnan, G., and Ponzoni, M. (2006) *J. Natl. Cancer Inst.* **98,** 1142–1157
11. Armstrong, M. B., Schumacher, K. R., Mody, R., Yanik, G. A., Opipari, A. W., Jr., and Castle, V. P. (2008) *J. Exp. Ther. Oncol.* **7,** 135–145
12. Obexer, P., Geiger, K., Ambros, P. F., Meister, B., and Ausserlechner, M. J. (2007) *Cell Death Differ.* **14,** 534–547
13. Ausserlechner, M. J., Obexer, P., Deutschmann, A., Geiger, K., and Kofler,

R. (2006) *Mol. Cancer Ther.* **5,** 1927–1934
14. Hemann, M. T., Zilfou, J. T., Zhao, Z., Burgess, D. J., Hannon, G. J., and Lowe, S. W. (2004) *Proc. Natl. Acad. Sci. U.S.A.* **101,** 9333–9338
15. Ausserlechner, M. J., Obexer, P., Geley, S., and Kofler, R. (2005) *Leukemia* **19,** 1051–1057
16. Ausserlechner, M. J., Obexer, P., Böck, G., Geley, S., and Kofler, R. (2004) *Cell Death Differ.* **11,** 165–174
17. Colell, A., Ricci, J. E., Tait, S., Milasta, S., Maurer, U., Bouchier-Hayes, L., Fitzgerald, P., Guio-Carrion, A., Waterhouse, N. J., Li, C. W., Mari, B., Barbry, P., Newmeyer, D. D., Beere, H. M., and Green, D. R. (2007) *Cell* **129,** 983–997
18. Engels, I. H., Stepczynska, A., Stroh, C., Lauber, K., Berg, C., Schwenzer, R., Wajant, H., Jänicke, R. U., Porter, A. G., Belka, C., Gregor, M., Schulze-Osthoff, K., and Wesselborg, S. (2000) *Oncogene* **19,** 4563–4573
19. Stepczynska, A., Lauber, K., Engels, I. H., Janssen, O., Kabelitz, D., Wesselborg, S., and Schulze-Osthoff, K. (2001) *Oncogene* **20,** 1193–1202
20. Nencioni, A., Hua, F., Dillon, C. P., Yokoo, R., Scheiermann, C., Cardone, M. H., Barbieri, E., Rocco, I., Garuti, A., Wesselborg, S., Belka, C., Brossart, P., Patrone, F., and Ballestrero, A. (2005) *Blood* **105,** 3255–3262
21. Chen, L., Willis, S. N., Wei, A., Smith, B. J., Fletcher, J. I., Hinds, M. G., Colman, P. M., Day, C. L., Adams, J. M., and Huang, D. C. (2005) *Mol. Cell* **17,** 393–403
22. Obexer, P., Hagenbuchner, J., Rupp, M., Salvador, C., Holzner, M., Deutsch, M., Porto, V., Kofler, R., Unterkircher, T., and Ausserlechner, M. J. (2009) *J. Biol. Chem.* **284,** 30933–30940
23. Labi, V., Erlacher, M., Kiessling, S., and Villunger, A. (2006) *Cell Death Differ.* **13,** 1325–1338
24. Villunger, A., Michalak, E. M., Coultas, L., Müllauer, F., Böck, G., Ausserlechner, M. J., Adams, J. M., and Strasser, A. (2003) *Science* **302,** 1036–1038
25. Orlowski, R. Z., and Kuhn, D. J. (2008) *Clin. Cancer Res.* **14,** 1649–1657
26. He, Q., Huang, Y., and Sheikh, M. S. (2004) *Oncogene* **23,** 2554–2558
27. Fennell, D. A., Chacko, A., and Mutti, L. (2008) *Oncogene* **27,** 1189–1197
28. Ding, W. X., Ni, H. M., Chen, X., Yu, J., Zhang, L., and Yin, X. M. (2007) *Mol. Cancer Ther.* **6,** 1062–1069
29. Zaman, F., Menendez-Benito, V., Eriksson, E., Chagin, A. S., Takigawa, M., Fadeel, B., Dantuma, N. P., Chrysis, D., and Sävendahl, L. (2007) *Cancer Res.* **67,** 10078–10086
30. Bui, N. T., Livolsi, A., Peyron, J. F., and Prehn, J. H. (2001) *J. Cell Biol.* **152,** 753–764
31. Satou, Y., Nosaka, K., Koya, Y., Yasunaga, J. I., Toyokuni, S., and Matsuoka, M. (2004) *Leukemia* **18,** 1357–1363
32. Oda, E., Ohki, R., Murasawa, H., Nemoto, J., Shibue, T., Yamashita, T., Tokino, T., Taniguchi, T., and Tanaka, N. (2000) *Science* **288,** 1053–1058
33. Motoyama, N., Wang, F., Roth, K. A., Sawa, H., Nakayama, K., Nakayama, K., Negishi, I., Senju, S., Zhang, Q., and Fujii, S. (1995) *Science* **267,** 1506–1510
34. Dole, M. G., Jasty, R., Cooper, M. J., Thompson, C. B., Nuñez, G., and Castle, V. P. (1995) *Cancer Res.* **55,** 2576–2582
35. Willis, S. N., Chen, L., Dewson, G., Wei, A., Naik, E., Fletcher, J. I., Adams, J. M., and Huang, D. C. (2005) *Genes Dev.* **19,** 1294–1305
36. Gomez-Bougie, P., Wuillème-Toumi, S., Ménoret, E., Trichet, V., Robillard, N., Philippe, M., Bataille, R., and Amiot, M. (2007) *Cancer Res.* **67,** 5418–5424